Using deep learning for automatic detection and segmentation of carbonate microtextures

Claire Birnie, and Viswasanthi Chandra, KAUST*

SUMMARY

The difficulties involved in studying micrometer- sized micrite crystals, and quantifying the associated impact on large scale geophysical properties, have long hindered our society's understanding of both Middle Eastern and global microporous limestones. Instance segmentation procedures, from the field of deep learning, offer the ability to identify at a pixel-level each individual crystal within an SEM image, allowing for automated morphological analysis. We illustrate how the common Masked Region-based Convolution Neural Network from computer vision can be adapted to the task of identifying individual micrite crystal within gray-scale SEM images. Leveraging Transfer Learning, the ResNet50 neural architecture is used with weights initialized through a pre-training on Microsoft's Common Objects in COntext (COCO) dataset. The resulting model accurately detects and separates a number of crystals observed within different SEM images. However the trained model is also shown to be highly susceptible to noise introduced as part of the imaging procedure, for example charging noise. Future work will aim to make the procedure more robust, reducing the impact of noise by adapting the pre-processing workflow and incorporating more noisy images into the training dataset.

INTRODUCTION

Microporosity accounts for a significant portion of total porosity in the Jurassic and Cretaceous limestone formations that host the super-giant hydrocarbon reservoirs in the Middle-East. A vast majority of microporosity in these formations is hosted within variably dense framework of microcrystalline calcite, aka micrite, which is also the origin for the term 'micritic carbonates'. The crystallometry and morphology of micrite crystals exerts a strong control on the distribution and nature of microporosity, and the associated rock mechanical and geophysical properties (Regnet et al., 2019; Chandra et al., 2021).

One of the main reasons why microporous limestones are poorly understood, in the Middle-East and across the world, is the technical difficulties involved in the study of micrometer-sized micrite crystals, and quantify the associated impact on large scale geophysical properties. Indeed, a number of previous studies have used Scanning Electron Microscopy (SEM) imagery to characterize micrite, qualitatively (Lambert et al., 2006; Kaczmarek et al., 2015) and quantitatively (Deville de Periere et al., 2011; Ramdani et al., 2021). However, there is still a lack of systematic research efforts to rapidly identify and classify micrite using SEM imagery. Recent advances in digital image analysis using machine learning methods provide a promising way forward to resolve this critical gap.

In this study, we investigate the application of state-of-the art deep learning techniques for identification and classification of micritic microtextures using SEM imagery. We evaluate segmentation methods potentially suitable for automated analysis of grey-scale SEM images of broken samples, which expose micrite crystal morphology. We demonstrate the application of Masked Region-based, Convolutional Neural Network (Mask-R CNN) for detection and classification of micrite crystals.

DATA

Collection

In this study we used over 200 SEM images acquired at magnifications of 10000x and 15000x, using secondary-electron detector, which is most suitable for resolving micrite crystal morphology. The SEM images were taken of broken samples prepared from over 100 core plugs drilled from 35 meters of Upper Jurassic Jubayla Formation outcrop cores from Saudi Arabia. The Jubayla Formation strata outcropping in the South-West of Riyadh are stratigraphically equivalent to the prolific Arab-D reservoir zones in the super-giant hydrocarbon fields of Eastern Saudi Arabia. The lithofacies associations in this formation have been well described in previous studies (Chandra et al. 2021), and are mainly composed of alternating grainstone-packstone channel facies and bioturbated mudstone-wackestone facies. Thin-section and SEM analysis suggests extensive micritization in this formation, associated with porous and non-porous micrite, as well as recrystallization.

Processing and labelling

The SEM image pre-processing included removal of data bar, followed by histogram equalization and non-local means filter, to improve the contrast of the image and minimize the background noise, respectively. The images were then exported for generating labels based on manual interpretation using the object identification feature in the open source AI tool makesense.ai. We used three types of labels to represent the main morphological attributes of micrite crystals; 1. Background (intercrystalline pore space) 2. Micrite and 3. Micrite boundary.

Splitting and augmentation

Deep learning techniques typically require large training datasets. Therefore, to increase the size of our training dataset, standard image augmentation procedures are implemented. However, prior to augmentation, ten images are retained as part of a blind, test dataset that is used to benchmark the final performance of the proposed procedure. Furthermore, to ensure no information leakage, the remaining images for training are separated 4 : 1 prior to augmentation with the first set, herein referred to as the training set, used for the training of the network. The second set, herein referred to as the validation set, is used for analyzing the performance of the network during its training.

The data augmentation workflow is performed on each image

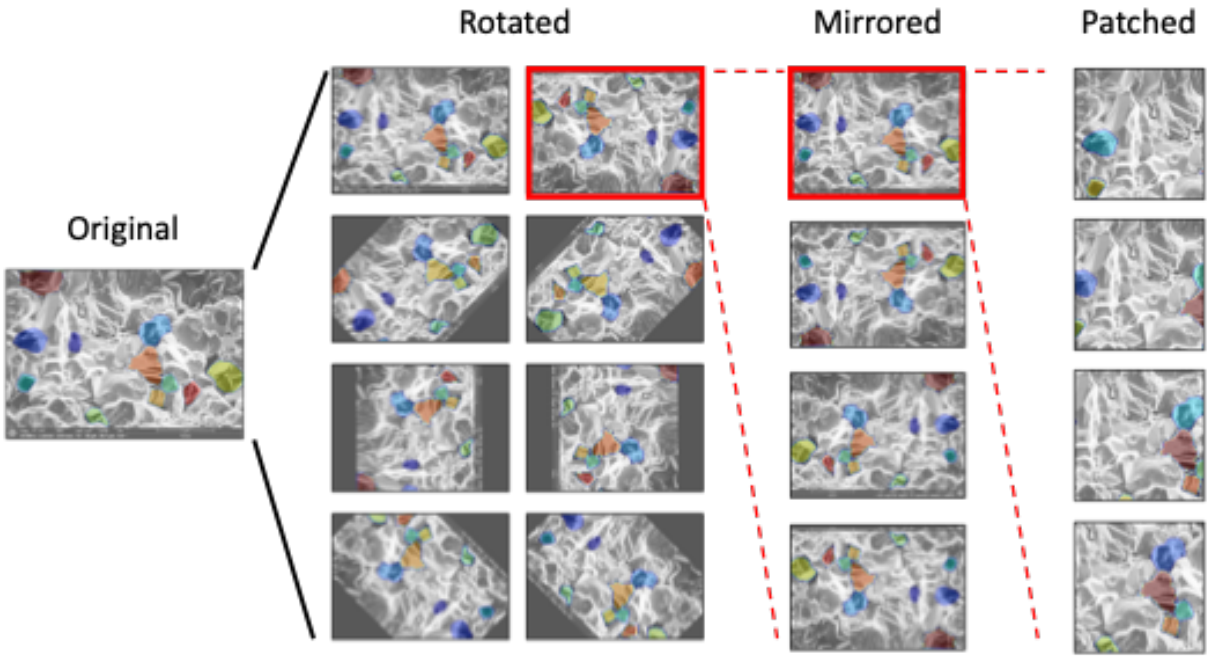

Figure 1: Data augmentation pipeline for training and valdiation data.

within the training and validation sets. The workflow is illustrated in Figure 1. To begin with, the images are rotated 45°, until a full circle is completed, increasing the data 8−fold. The rotated images then undergo mirroring on their horizontal and vertical axis, increasing the dataset a further 4−fold. Finally, ten random patches are extracted from each of the rotated-mirrored images. These patches are chosen to be of size 800 $\times$ 800, in comparison to the original image sizes which range from 954 $\times$ 1024 to 1094 $\times$ 1536. To be selected the patches must contain at least one crystal and cannot contain any significant edge effect from the rotation procedure. In the end, the training dataset contains 6168 patches, while the validation dataset contains 1296 patches.

SEGMENTATION METHODOLOGY

The aim of this study is to investigate techniques for automatic segmentation of individual micrite crystals within an SEM image. In other words, we are striving to detect which pixels within an SEM image correspond to which crystals. Figure 2 illustrates the different deep learning techniques for object classification, detection and segmentation. An instance-segmentation approach is chosen for this study due to it's ability to detect and separate individual crystals at a pixel-level.

The Masked Region-based, Convolutional Neural Network (Mask R-CNN) of He et al. (2017), is consistently one of the top performing networks in image challenges. A number of studies have utilised it, either in a partially trained or fully re-initialised fashion, for instance-segmentation tasks across a range of different scientific fields. For example, Malbog (2019) utilise the Mask R-CNN for pedestrian detection for autonomous vehicles, Chiao et al. (2019) employ the same procedure in the field of medical imaging for breast cancer detection, and Xu et al. (2020) leverage the Mask R-CNN framework for live stock counting. In this study, the common ResNet50 architecture is used combined with a Feature Pyramid Network (FPN) (Lin et al., 2017) which forms the backbone of the network for identifying Regions Of Interests (ROIs).

Transfer learning offers the ability to use knowledge gained through the training of a network (for a specific task and dataset) as the starting point for training the network for a new task and/or dataset (Pan and Yang, 2009). Transfer learning has been shown to significantly speed up training times (e.g., George et al., 2018), as well as improve results where only a few training samples are available (e.g., Cunha et al., 2020). As an initial investigation, we consider the performance of the network when initialised with the weights from pre-training on the Common Objects in COntext (COCO) dataset. (The weights are available via the PyTorch software package.) The COCO dataset, of Lin et al. (2014), is composed of more than 200k labelled images and is one of the most-widely used benchmarking datasets for computer vision tasks. The network is trained for a further 100 epochs on our SEM data, using Stochastic Gradient Descent as the optimiser with a momentum of 0.9. A variable learning rate is employed with a decay factor of 0.1, and the data are handled as mini-batches of size 32.

RESULTS AND DISCUSSION

Figure 3 illustrates the trained model applied to four hold-out images that the network was not exposed to during training. The different colours in the second and third columns represent

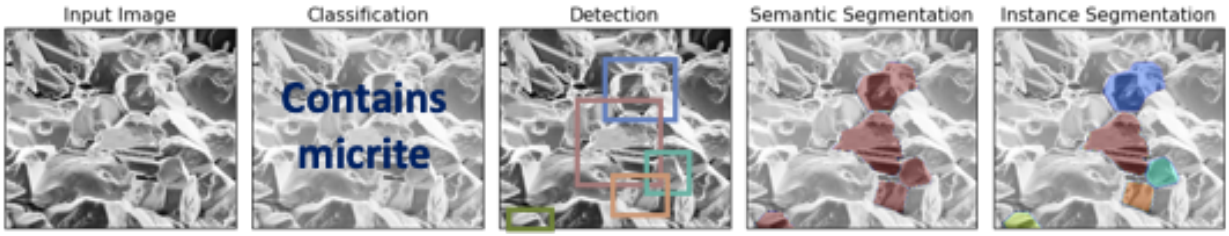

Figure 2: Different deep learning procedures which could be used for analysis of crystals within SEM images.

the different crystals detected within the image.

A number of promising features can be observed from the identified crystals. For example, in Figure 3(a) the network was able to distinguish between the micrite crystals and the recrystallized neomorphic calcite. Another promising aspect of the results is that, as observed in Figure 3(c), the network accurately distinguishes porous micrite, which are rounded to subhedral, from non-porous anhedral compact micrite.

However, despite the promising initial results, the results are not perfect and there is clear room for improvement. For instance, in Figure 3(a) we hoped to identify the crystal that bridges between the blue and teal crystals in the bottom left corner. We hypothesise that this may have been missed due to the contrast between this unidentified crystal and its neighbours being relatively low. Future work will incorporate contrast normalisation into the pre-processing procedure prior to training the network to try reduce the number of such crystals remaining undetected.

The presence of charging noise - clearly observed in Figure 3(d) - has noticably limited the performance of the segmentation procedure. This linearly-correlated noise has resulted in a very poor performance of the network, highlighting the susceptibility of the network to noise. There are two approaches we could take to mitigate this effect, the first would be to incorporate more samples with charging noise into the training samples to try teach the network to handle such noise without degrading the detection performance. An alternative would be to incorporate a denoising procedure into the pre-processing pipeline. This denoising procedure could be a more conventional approach such as the application of a wavelet filter (e.g., Sun et al., 2009) or it could involve newer deep learning procedures such as self-supervised, blind-spot networks as illustrated by Krull et al. (2019), Birnie et al. (2021) and Liu et al. (2022). Such self-supervised networks require no noisy-clean training data pairs and are therefore not burdened by the same limitations as standard, supervised denoising procedures.

Another challenge faced in this work, and in many other applications of deep learning in geoscience, is the level of human subjectivity involved in the labelling of the data for training. For example, what one interpreter may classify as a crystal, another may not. Similarly, it is also very difficult for an interpreter to be fully consistent between images when annotating. Whilst not yet solved, a number of solutions have been proposed to tackle this phenomenon, known as Label Bias. The most common approach involves re-weighting the data samples, without re-labelling the data (Ren et al., 2018; Jiang and Nachum, 2020; Lahoti et al., 2020). Prior to employing such a scheme we shall run a sensitivity study similar to Rolnick et al. (2017) to understand the level of bias within our labels and its influence on the network.

Finally, in this study we have leveraged transfer-learning to provide initial weights for the network, under the assumption that the network learnt to detect edges and shapes in images based on the data is was previously trained on. If correctly assumed, and the properties between our SEM images do not drastically vary to the properties of the natural images in the COCO dataset, then the training time should have been reduced in comparison to training the network from randomly initialised weights. To test this assumption, in future work we shall train the same network architecture with randomly initialised weights and compare it to the trained network from this study.

CONCLUSION

Initial results have indicated that the Mask R-CNN approach provides great promise in the automatic identification of individual crystals at a pixel-level. Individual crystal identification at a pixel level (as opposed to semantic segmentation or bounding box detection) enables the quantification of micrite morphological features, such as shape, size and relative distributions. Such a quantitative analysis would ultimately allow us to evaluate their impact on rock mechanical and geophysical properties at the reservoir scale. Whilst not yet perfect, we have shown how a neural network can be trained to detect individual crystals with a wide range of morphological features on a relatively small training dataset, ~ 200 images. Future work shall investigate how to further improve the networks performance, in particular focusing on identifying the optimum pre-processing workflow.

ACKNOWLEDGMENTS

For computer time, this research used the resources of the Supercomputing Laboratory at King Abdullah University of Science & Technology (KAUST) in Thuwal, Saudi Arabia.

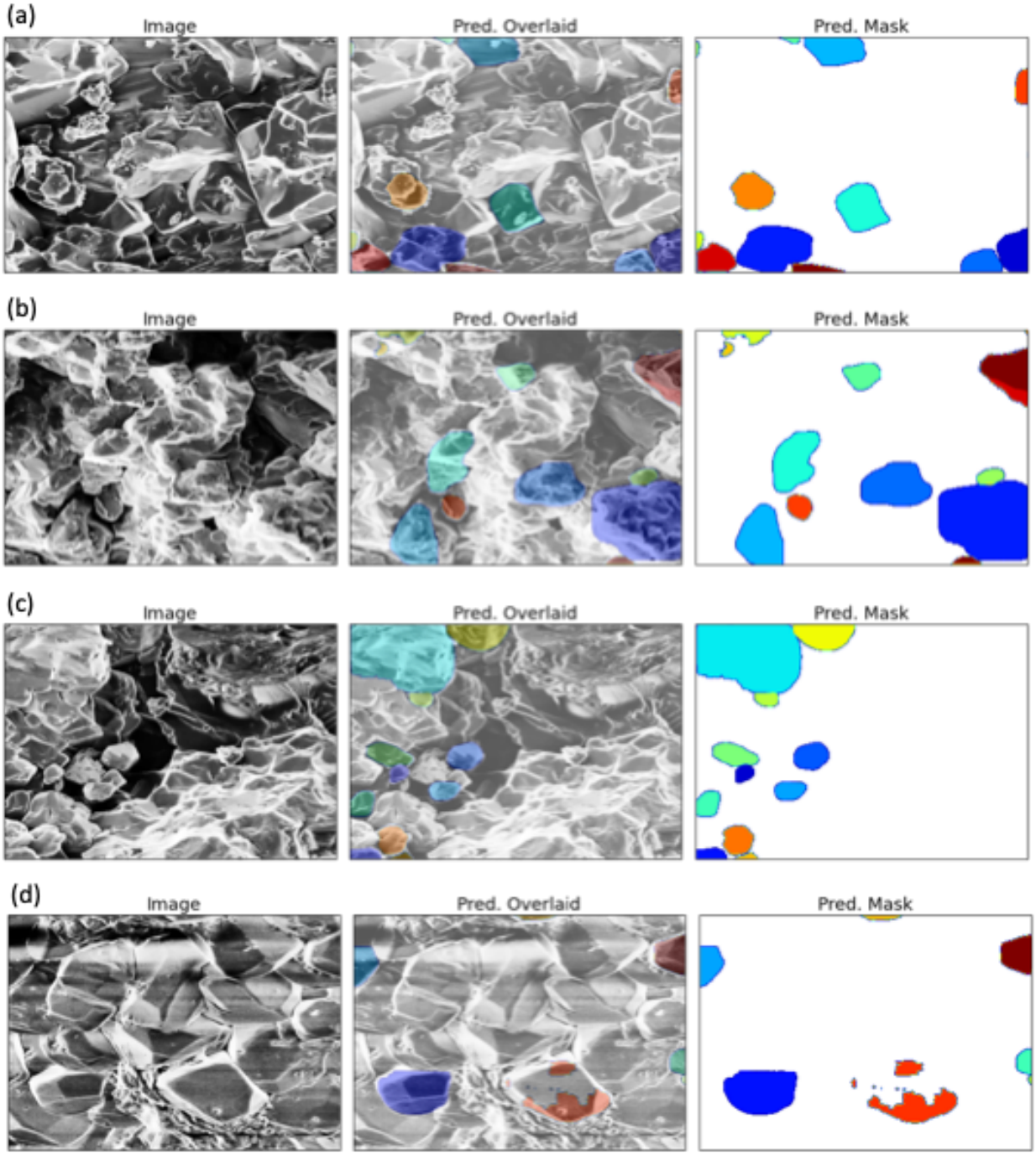

Figure 3: Examples of the trained network applied to different hold-out images. Colours indicate the different individual crystals identified.

10.1190/image2022-3751305.1

REFERENCES

Birnie, C., M. Ravasi, S. Liu, and T. Alkhalifah, 2021, The potential of self-supervised networks for random noise suppression in seismic data: Artificial Intelligence in Geosciences, **2**, 47–59.

Chandra, V., A. Petrovic, P. Khanna, A. I. Ramdani, B. Yalcin, V. Vahrenkamp, and T. Finkbeiner, 2021, Impact of depositional and diagenetic features on petrophysical and rock mechanical properties in Arab-D reservoir equivalent Upper Jubaila Formation, Saudi Arabia: Marine and Petroleum Geology, **129**, 105076, doi: https://doi.org/10.1016/j.marpetgeo.2021.105076.

Chiao, J.-Y., K.-Y. Chen, K. Y.-K. Liao, P.-H. Hsieh, G. Zhang, and T.-C. Huang, 2019, Detection and classification the breast tumors using mask R-CNN on sonograms: Medicine, 98.

Cunha, A., A. Pochet, H. Lopes, and M. Gattass, 2020, Seismic fault detection in real data using transfer learning from a convolutional neural network pre-trained with synthetic seismic data: Computers & Geosciences, **135**, 104344, doi: https://doi.org/10.1016/j.cageo.2019.104344.

de Periere, M. D., C. Durlet, E. Vennin, L. Lambert, R. Bourillot, B. Caline, and E. Poli, 2011, Morphometry of micrite particles in cretaceous microporous limestones of the middle east: Influence on reservoir properties: Marine and Petroleum Geology, **28**, 1727–1750, doi: https://doi.org/10.1016/j.marpetgeo.2011.05.002.

George, D., H. Shen, and E. Huerta, 2018, Classification and unsupervised clustering of LIGO data with deep transfer learning: Physical Review D, **97**, 101501, doi: https://doi.org/10.1103/PhysRevD.97.101501.

He, K., G. Gkioxari, P. Dollár, and R. Girshick, 2017, Mask R-CNN: Proceedings of the IEEE International Conference on Computer Vision, 2961–2969.

Jiang, H., and O. Nachum, 2020, Identifying and correcting label bias in machine learning: International Conference on Artificial Intelligence and Statistics, PMLR, 702–712.

Kaczmarek, S. E., S. M. Fullmer, and F. J. Hasiuk, 2015, A universal classification scheme for the microcrystals that host limestone microporosity: Journal of Sedimentary Research, **85**, 1197–1212, doi: https://doi.org/10.2110/jsr.2015.79.

Krull, A., T.-O. Buchholz, and F. Jug, 2019, Noise2voidlearning denoising from single noisy images: Proceedings of the IEEE/CVF Conference on Computer Vision and Pattern Recognition, 2129–2137.

Lahoti, P., A. Beutel, J. Chen, K. Lee, F. Prost, N. Thain, X. Wang, and E. Chi, 2020, Fairness without demographics through adversarially reweighted learning: Advances in Neural Information Processing Systems, **33**, 728–740, doi:

Lambert, L., C. Durlet, J. P. Loreau, and G. Marnier, 2006, Burial dissolution of micrite in Middle East carbonate reservoirs (Jurassic-Cretaceous): Keys for recognition and timing: Marine and Petroleum Geology, **23**, 79–92, doi: https://doi.org/10.1016/j.marpetgeo.2005.04.003.

Lin, T.-Y., P. Dollár, R. Girshick, K. He, B. Hariharan, and S. Belongie, 2017, Feature pyramid networks for object detection: Proceedings of the IEEE Conference on Computer Vision and Pattern Recognition, 2117–2125.

Lin, T.-Y., M. Maire, S. Belongie, J. Hays, P. Perona, D. Ramanan, P. Dollár, and C. L. Zitnick, 2014, Microsoft coco: Common objects in context: European Conference on Computer Vision, Springer, 740–755.

Liu, S., C. Birnie, and T. Alkhalifah, 2022, Coherent noise suppression via a self-supervised deep learning scheme: 84th Annual International Conference and Exhibition, EAGE, Extended Abstracts, doi: https://doi.org/10.3997/2214-4609.202210382.

Malbog, M. A., 2019, Mask R-CNN for pedestrian crosswalk detection and instance segmentation: IEEE 6th International Conference on Engineering Technologies and Applied Sciences.

Pan, S. J., and Q. Yang, 2009, A survey on transfer learning: IEEE Transactions on Knowledge and Data Engineering, **22**, 1345–1359, doi: https://doi.org/10.1109/TKDE.2009.191.

Ramdani, A., T. Finkbeiner, V. Chandra, P. Khanna, S. Hanafy, and V. Vahrenkamp, 2021, Multiattribute probabilistic neural network for near-surface field engineering application: The Leading Edge, **40**, 794–804., doi: https://doi.org/10.1190/tle40110794.1.

Regnet, J. B., C. David, P. Robion, and B. Menéndez, 2019, Microstructures and physical properties in carbonate rocks: A comprehensive review: Marine and Petroleum Geology, **103**, 366–376, doi: https://doi.org/10.1016/j.marpetgeo.2019.02.022.

Ren, M., W. Zeng, B. Yang, and R. Urtasun, 2018, Learning to reweight examples for robust deep learning: International Conference on Machine Learning, PMLR, 4334–4343.

Rolnick, D., A. Veit, S. Belongie, and N. Shavit, 2017, Deep learning is robust to massive label noise: arXiv preprint, arXiv:1705.10694.

Sun, W., J. A. Romagnoli, J. W. Tringe, S. E. Létant, P. Stroeve, and A. Palazoglu, 2009, Line edge detection and characterization in SEM images using wavelets: IEEE Transactions on Semiconductor Manufacturing, **22**, 180–187, doi: https://doi.org/10.1109/TSM.2008.2011174.

Xu, B., W. Wang, G. Falzon, P. Kwan, L. Guo, G. Chen, A. Tait, and D. Schneider, 2020, Automated cattle counting using mask R-CNN in quadcopter vision system: Computers and Electronics in Agriculture, **171**, 105300, doi: https://doi.org/10.1016/j.compag.2020.105300.